Journal of Molecular Liquids 352 (2022) 118724

Contents lists available at ScienceDirect

Journal of Molecular Liquids

journal homepage: www.elsevier.com/locate/molliq

Quality by design assisted optimization of temozolomide loaded PEGylated lyotropic liquid crystals: Investigating various formulation and process variables along with in-vitro characterization

Tejashree Waghule [1], K. Laxmi Swetha, Aniruddha Roy, Ranendra Narayan Saha, Gautam Singhvi [1,*]

Industrial Research Laboratory, Department of Pharmacy, Birla Institute of Technology and Science, Pilani, Pilani Campus, India

ARTICLE INFO

Article history:
Received 19 November 2021
Revised 5 February 2022
Accepted 7 February 2022
Available online 11 February 2022

Keywords:
Box Behnken design
Hemolysis
Liquid crystals
PEGylation
Stability
Temozolomide

ABSTRACT

Temozolomide (TMZ) is approved for the treatment of glioblastoma. The objective of the present study was to develop and characterize TMZ loaded lyotropic liquid crystals (LLCs) for intravenous delivery. Various formulation and process variables were studied in detail, following the quality by design principles. A three-level Box Behnken design was used for optimization. The effect of lipid concentration, surfactant concentration, and co-surfactant concentration on response variables like size, size distribution, zeta potential, entrapment efficiency, and drug loading was investigated using the statistical data obtained by Design Expert® software. The results demonstrated that LLCs were obtained in the size range of 53.15–186.50 nm with PDI less than 0.25. The optimized formulation showed particle size of 97.70 ± 0.481 nm and entrapment efficiency of 36.46 ± 1.48%. TMZ loaded LLCs were found to follow Korsmeyer's Peppas model and showed sustained release up to 72 h. The LLCs were further PEGylated to prevent hemolysis and achieve long plasma circulation. PEGylated LLCs showed less than 5% hemolysis. TMZ loaded LLCs demonstrated higher cytotoxicity towards glioma cell lines as compared to native TMZ. The results revealed that the prepared LLCs could be a potential delivery system to enhance the efficacy of TMZ. Additionally, the preparation method involved a minimum number of steps ensuring reproducibility and scalability.

1. Introduction

Temozolomide (TMZ) is an imidazotetrazine derivative approved by the United States Food and Drug Administration (USFDA) for treating brain cancer, especially glioblastoma. It is a small molecule amphiphilic in nature belonging to Class I. TMZ is marketed as oral capsules and powder to be reconstituted for intravenous administration. Despite 100% oral bioavailability, only 20–30% of the drug is available to the brain due to its pH-dependent instability and short half-life (1.8 h). In plasma (at pH 7.4), it undergoes spontaneous opening of the tetrazine ring to 5-(3-methyltriazen-1-yl) imidazole-4-carboxamide (MTIC). This MTIC has a short half-life (~2.5 min) attributed to hydrolysis to 5-amino-imidazole-4-carboxamide (AIC) and a methyl diazonium ion. These metabolites are responsible for the alkylating action of the drug; however, they cannot pass through the blood-brain barrier due to their hydrophilic nature. Thus, a higher dose of the drug needs to be administered, leading to myelosuppression, thrombocytopenia, or neutropenia [1–3]. Therefore, there is a need to develop a formulation to overcome the existing issues. Encapsulating TMZ within nanoparticles can prevent plasma exposure, provide controlled release, provide longer circulation time, and improve its concentration in the brain. Also, reduction of the dose may improve patient compliance. Although various nanoformulations like polymeric nanoparticles, solid lipid nanoparticles, nanostructured lipid carriers, and liposomes have been investigated [4,5], complex composition, sophisticated process, and poor entrapment of TMZ within these nanoparticles remain a challenging task.

Lyotropic Liquid Crystals (LLCs) have gained much attraction in recent years in the field of pharmaceutical nanotechnology due to their unique structural properties. LLCs exhibit highly ordered structural alignment and optical properties similar to solid crystals. Additionally, they exhibit fluidity, surface tension, and viscosity like a liquid. LLCs composition consists of lipidic amphiphiles such as glyceryl monooleate (GMO) and lecithin that self-assemble into different three-dimensional structures with aqueous channels when added into excess of the aqueous medium. Stabiliz-

* Corresponding author.
E-mail address: gautam.singhvi@pilani.bits-pilani.ac.in (G. Singhvi).
[1] Authors contributed equally.

https://doi.org/10.1016/j.molliq.2022.118724
0167-7322/

ers like Pluronics and polyethylene glycol derivatives are essential for forming stable structures. When added into the water, these lipids align themselves at the air-water interface with hydrophilic heads towards the water and lipophilic tails towards the air. As the lipid concentration increases, lipid molecules start moving into the water phase as there is no space to accommodate more molecules at the interface. When the equilibrium is reached (critical micelle concentration), these molecules align as micelles. Further increase in concentration leads to the formation of various three-dimensional structures like cubic, lamellar or hexagonal [6,7].

The presence of varying polarities in the LLCs region favors entrapment of hydrophobic, lipophobic as well as amphiphilic drug molecules [8,9]. The presence of multiple layers consisting of a honeycomb-like structure allows the entrapped drug to diffuse slowly through the LLCs structure, providing extended drug release. GMO is the most common LLCs forming lipid. It is biocompatible, biodegradable, and classified as GRAS (generally recognized as safe). However, it is reported to cause hemolysis on parenteral administration. Surface coating of the LLCs with polyethylene glycol (PEG) derivatives provides several advantages like improving hemocompatibility, reducing immunogenicity, preventing uptake by the reticuloendothelial system, and providing longer circulation time in plasma [10–12].

In the present study, for the first time, the LLCs were formulated to administer TMZ intravenously to improve the plasma circulation time. The TMZ loaded LLCs were formulated employing the fundamentals of Quality by Design (QbD). The process for LLCs preparation was simple, solvent-free, and feasible for industrial applicability. To obtain the design space, various formulation and process parameters were studied in detail. Further, the LLCs were PEGylated to prevent hemolysis on systemic administration.

2. Materials

Glyceryl monooleate (Mono ester content: minimum 35%, Free Glycerin: maximum 7%) (Monegyl-O100) was received as a gift sample from Mohini Organics Pvt. Ltd. Pluronic F- 127 was acquired as a gift sample from BASF (Mumbai), Polyethylene glycol 200 (PEG 200) was purchased from CDH Fine Chemicals (New Delhi). DSPE-PEG 2000 was obtained as a gift sample from Lipoid. Temozolomide was obtained as a gift sample from Biophore India Pharmaceuticals Pvt. Ltd, Hyderabad, India.

3. Methods

3.1. Optimization of TMZ loaded LLCs using quality by design (QbD) approach

3.1.1. Defining and identifying quality target product profile and critical quality attributes

Formulating a product using the fundamentals of QbD begins with defining the Quality Target Product Profile (QTPP). It majorly describes various aspects of the formulation related to its safety, efficacy, and quality. QTPP summarizes the characteristics which are desirable in the target product. From the QTPP, the critical and non-critical attributes are distinguished based on the impact and severity analysis. Critical quality attributes (CQAs) are those properties of the formulation that are expected to be within an appropriate range to ensure the overall quality of the final product. Once the CQAs are identified, the formulation scientist can investigate them further in detail [13,14].

3.1.2. Quality risk management

Risk assessment (identification and analysis) was conducted to minimize the risks to product quality. Inadequate information related to risks might result in product failure. Ishikawa fishbone diagram was designed to recognize various risk factors. Various causes (material attributes and process parameters) that are likely to affect the outcome were recognized. A relationship between the CQAs and material attributes (MAs) along with the process parameters (PPs) was obtained [15,16]. The relative risk-based matrix analysis (RRMA) was employed to categorize the risk into low, medium, and high potential [17].

3.1.3. Identifying critical material attributes (CMAs) and critical process parameters (CPPs)

Screening of various factors was done in the initial preliminary experiments. The critical material attributes related to the drug and excipients were distinguished from the non-critical attributes. Similarly, the critical process parameters were also identified. Failure mode effect analysis (FMEA) was used to assess the risk based on probability of occurrence, severity, and detectability. Based upon the findings, risk priority numbers (RPN) were assigned to these material attributes and process parameters (Equation 1). The factors with RPN scores higher than 25 were considered critical and further evaluated for optimization [18].

$$RPN\,score = Severity \times Detectibility \times Occurrence \quad (1)$$

3.1.4. Preparation of TMZ loaded LLCs

During the formulation of TMZ loaded LLCs, various preparation and size reduction methods were explored to understand the effect on the particle size and entrapment efficiency. Initially, a desired quantity of GMO, Poloxamer 127, PEG 200, and TMZ were transferred to a clean vial. The lipid phase was melted at around 70 ± 5 °C on a hot plate. Acetone was used as a solvent to dissolve TMZ in the lipid phase. Separately, the purified water was heated and maintained at the same temperature. The lipid phase was added to the water phase under mechanical stirring, which was further continued for 10 min. In the following method, instead of acetone, water itself was used as a solvent for drug solubilization and mesophase formation. A weighed amount of TMZ was dissolved in a specified quantity of water based on the maximum solubility of TMZ in water (5 mg/ mL). This was heated to 70 ± 5 °C and added drop-wise to the melted lipid phase under magnetic stirring (500 rpm, 5 min). The formed phase was cooled down to room temperature to allow mesophase formation and entrapment of TMZ within. The remaining quantity of water was added to the formed phase. This was immediately followed by size reduction using probe sonication for 2 min at 20% amplitude (30 s Pulse ON and 10 s Pulse OFF cycle) [9,19].

The optimized formulation was further PEGylated by replacing PEG 200 with DSPE-PEG 2000. Various percentage of DSPE-PEG 2000 (0.05%, 0.1%, 0.25%, 0.5% and 1% of the total dispersion) were screened and the effect on size distribution and zeta potential was evaluated. The best formulation was selected based on the hemolysis study [10,20].

3.1.5. Experimental design

Independent and response variables were decided based on the literature survey, prior experience, preliminary trials, and risk assessment. Based on the number of variables, the 'Box Behnken' design (BBD) was selected to obtain the optimized formulation and to study the effect of various formulation variables on the response variables. The Box Behnken design helps to predict the actual relation between the factors with a restricted number of experiments without compromising the resulting quality [21]. The higher and lower levels of the formulation variables were decided based on the preliminary experiments. The Design Expert® software (Version 13, Stat-Ease Inc.) was used to obtain the trials. Accordingly, the formulation trials were taken and characterized.

The values obtained were entered in the software as response variables. The effect of various variables was further studied statistically [22].

3.1.6. Data analysis

The data were analyzed statistically by the software. The software states the significant and non-significant terms based on statistical analysis (F-value and p-value). The non-significant terms were excluded from the model. The best model was selected based on various factors. The values of Predicted R^2 must not be negative. The difference between the Predicted R^2 and Adjusted R^2 should be less than 0.2. denote the significant and non-significant terms. The PRESS value helps to select the best model for each response. The Adequate precision value should be more than 4. After obtaining a significant model, Polynomial equations were generated by the software. The equation provides the relationship between the response variable and the independent variable. Further, the data were analyzed using different diagnostic and model graphs [23].

3.1.7. Validation of the design and establishment of design space

After obtaining the significant model equations for each response, the target goals were set in the software, and various solutions were obtained. Three random solutions were selected for validating the model equations. The predicted and observed values of the responses were compared. An optimized composition was selected based on the desired particle size, highest entrapment efficiency, low lipid concentration, and the desirability value near to 1 [24,25]. Design space was established to get a range of formulation variables to achieve the desired set of response variables [26].

3.2. Characterization of TMZ loaded LLCs

3.2.1. Particle size, Polydispersity index (PDI), and zeta potential

Dynamic light scattering technique was utilized to measure the size distribution, and surface charge of the prepared TMZ loaded LLCs. The particle size was represented as diameter values in nanometers (d.nm). The measurements were conducted using Zetasizer (Zetasizer Nano-ZS ZEN 3600, Malvern) instrument. It used a red laser (633 nm wavelength) and 173° scattering angle. Before analysis, the formulation was diluted up to 10 times with Milli-Q water. The analysis of each formulation was conducted in triplicates at 25 °C temperature [27,28].

3.2.2. Entrapment efficiency (% EE) and drug loading (% DL)

The % EE was calculated by the dialysis bag technique. A 1 mL TMZ loaded LLCs dispersion was filled into the dialysis bag and tied at both ends using thread. The bag was dispersed into pH 4.5 acetate buffer (50 mL) with constant magnetic stirring at 80 rpm for 45 min to separate the free drug. Thereafter, the formulation was subjected to lysis using methanol. The dispersion was centrifuged at 10,000 rpm for 15 min at 4 °C to settle the lipid. The supernatant was analysed for drug content using an in-house developed validated HPLC method. The amount of drug entrapped and drug loading in the TMZ loaded LLCs was determined by Equations 2 and 3, respectively [29].

$$\%Entrapment\ efficiency = \frac{Amount\ of\ drug\ entrapped}{Total\ amount\ of\ drug\ added} * 100 \quad (2)$$

$$\%Drug\ Loading = \frac{Amount\ of\ drug\ entrapped}{Total\ weight\ of\ excipients} * 100 \quad (3)$$

3.2.3. Morphology

A thin film of TMZ loaded LLCs dispersion was formed on a glass slide with the aid of vacuum drying. The morphology was studied under the Polarized light microscope (Olympus: BX53M) with objective 20× magnification. The samples were observed under a cross polarizer and without a cross polarizer [30]. The thin film of LLCs formed was also coated with gold (Gold sputter module, Quorum ES, UK) and observed under Field Emission Scanning Electron Microscopy (FESEM) (Apreo Switch XT microscope, USA) [31].

3.2.4. Attenuated total Reflectance-Fourier Transform-Infrared spectroscopy (ATR-FTIR)

FTIR study of TMZ, physical mixture, TMZ loaded LLCs, PEGylated LLCs dispersion, and optimized PEGylated TMZ loaded LLCs dispersion was performed using Bruker ATIR spectrophotometer (OPUS software). Spectrum was obtained in the wavelength range 4000–400 cm^{-1} [32].

3.2.5. X-ray diffraction (Powder XRD)

X-ray diffractogram of TMZ, physical mixture, and PEGylated TMZ loaded LLCs were obtained using the X-ray diffractometer (Rigaku-miniflex) with Cu (λ = 1.54) tube as an anode. The scanning speed was 1°/min, and the voltage was set at 30 kV. The diffractogram was obtained with a scattering angle (2θ) ranging between 10 and 40° [33].

3.2.6. Drug release and release kinetics

In-vitro drug release was studied with the dialysis bag technique. The drug stability and sink conditions were ensured during the entire study. Initially, the time taken for 100% TMZ diffusion was evaluated by filling the TMZ solution (1 mg/mL) into the dialysis bag (molecular cutoff – 12–14 kDa, Himedia). After which, the effect of drug loading on the release rate and the release kinetics was investigated. TMZ loaded LLCs formulation with different drug loading (B1- 0.45%, B2- 0.72%, B3- 1.00%, B4- 1.52%) were prepared. The particle size, PDI, and entrapment efficiency of all the formulations were constant. These were filled in the dialysis bag individually. The dialysis bags were then placed in 30 mL of acetate buffer (pH 4.5, 100 mM) for all the studies. The exposed area of the dialysis bag to the release media was 25 cm^2. The media was kept under magnetic stirring (80 rpm) at 37 ± 0.5 °C. Samples (0.5 mL) were withdrawn at different time points and analyzed using the developed HPLC method to obtain the concentration of TMZ released. The release profile was plotted (time vs. % cumulative drug release), which was further studied for release kinetics using DDSolver software (Excel Add-In). The best fit release model was identified based on the high R^2 value, highest MSC (Model Selection Criteria) value, and lowest AIC (Akaike Information Criterion) value [34–36]. The corresponding t_{25}, t_{50}, and t_{75} values were also obtained [37].

3.2.7. Hemolysis study

Nanoparticles administered into the systemic circulation are likely to interact with the blood components. A hemolysis study was conducted to evaluate the hemolytic toxicity of the prepared LLCs. Fresh blood was collected from Wistar rats into Eppendorf tubes containing 10% w/v EDTA (ethylenediamine-tetraacetic acid). The tubes were centrifuged at 1000 rpm for 5 min at 4 °C to obtain the red blood cells (RBCs) pellet. The obtained RBCs pellet was washed with 0.9% normal saline and again centrifuged at 1000 rpm for 5 min. The obtained pellet was resuspended in normal saline (1 mL to 5 mL). The study was conducted to evaluate hemolytic potential of LLCs, and PEGylated LLCs containing 0.05%, 0.1%, 0.25%, 0.5% and 1% DSPE-PEG 2000 of the total dispersion. Different dilutions (0, 2, 5, and 10 times) of all formulations were evaluated. Each formulation (100 µL) was added to 100 µL of the RBCs suspension in the 2 mL Eppendorf tubes. For positive and negative controls, instead of formulation, 1% Triton X and normal saline were added to the RBC suspension, respectively. The

tubes were incubated at 37 °C for 30 min. After which the volume was made up to 1 mL with normal saline and centrifuged at 1000 rpm for 5 min at 4 °C temperature to settle the intact RBCs. The absorbance of the supernatant was measured using the BioTek Epoch Microplate reader (Gen5™ 1.11 software) at 540 nm. The % hemolysis caused was calculated using Equation 4 [10,20,38].

$$\%Hemolysis = \frac{Sample\ absorbance - Negative\ control\ absorbance}{Positive\ control\ absorbance - Negative\ control\ absorbance} * 100 \quad (4)$$

3.2.8. In-vitro cytotoxicity study

In-vitro cytotoxicity of the formulations was analyzed against U-373 MG (a human glioblastoma astrocytoma) cells. U-373 MG cells were cultured in DMEM media (Gibco) supplemented with 10% fetal bovine serum (FBS, Himedia), 50 units/mL penicillin, and 50 mg/mL streptomycin (Thermo Fisher Scientific) maintained at 37 °C and 5% CO_2. Trypsin–EDTA (Thermo Fisher Scientific) solution (0.05%) was used to detach cells. The cytotoxicity of TMZ, blank LLCs, TMZ loaded LLCs and PEGylated LLCs was evaluated using the MTT (3-(4,5-dimethylthiazol-2-yl)-2,5-diphenyl-2H-tetrazolium bromide) assay. The glioma cells were seeded in 96 well plates at a density of 2×10^3 cells per well. The cells were incubated at 37 °C for 24 h to permit cell attachment. Thereafter, the cells were treated with TMZ, and LLCs formulations with TMZ concentration equivalent to 0.04, 0.2, and 1 mM. TMZ (10 mg/mL) stock solution was prepared in dimethyl sulfoxide (DMSO). Untreated cells were taken as control. After treatment for 72 h with formulations, the cells were incubated with MTT dye (5 mg/mL in culture media) for 4 h. The formed formazan crystals were solubilized by the addition of DMSO (200 μL) and the absorbance was measured at 570 and 630 nm using the BioTek Epoch Microplate reader (Gen5™ 1.11 software). The percentage of viable cells was calculated using equation 5 [20,39].

$$\%Cell\ viability = \frac{Sample_{abs}570nm - Sample_{abs}630nm}{Control_{abs}570nm - Control_{abs}630nm} * 100 \quad (5)$$

3.3. Reproducibility and scale-up studies

In order to check the industrial feasibility, reproducibility and scale-up studies were conducted. The optimized batch was repeated 6 times to confirm the reproducibility. The formulation was scaled up to 5 times (50 mL) of the initial batch volume (10 mL). For the 10 mL batch, a probe with 3 mm diameter was used, while for the 50 mL batch probe with 13 mm diameter was utilized. The process parameters were optimized by keeping the composition constant. The formulations were characterized for particle size and PDI.

It is expected that LLCs need to be diluted with suitable media for intravenous delivery in the form of infusion. LLCs are self-assembled systems that are likely to dissemble on dilution and release the entrapped drug. The stability on dilution is a critical factor for intravenous delivery. The prepared LLCs formulation was diluted 50, 100, 500, and 1000 times. The change in particle size and PDI was studied thereafter [40,41].

4. Results and discussion

4.1. Optimization of TMZ loaded LLCs using QbD approach

4.1.1. Identifying QTPP and CQAs

The QTPP for TMZ loaded LLCs was identified as represented in Supplementary Table 1. The CQAs were derived from the QTPP using impact and severity analysis a summarized in Table 1 [13,42].

4.1.2. Quality risk management

Various material attributes and process parameters identified were represented as the Ishikawa Fish Bone diagram (Fig. 1). The material attributes and process parameters were linked to the CQAs, and the severity of risk evaluated using the RRMA are represented in Table 2-4 [22,43].

4.1.3. Identifying critical material attributes (CMAs) and critical process parameters (CPPs)

Critical and non-critical factors were distinguished based on the RPN score. The solubility and chemical stability were found to be the CMAs related to TMZ (Table 5). The solubility in solvents and lipids was found to be a critical factor as it majorly affects the entrapment efficiency and drug release. TMZ has pH-dependent stability, thus chemical stability needs to be ensured during storage and when *in vivo*. The type and concentration of the lipid play a crucial role in forming the liquid crystal phase. The lipid may show concentration-dependent toxicity, which relates to the safety aspects. Surfactant concentration plays an essential role in stabilizing the liquid crystal phase. In the case of TMZ, the pH of the aqueous phase need to be ensured considering the stability. The CMAs related to excipients are represented in Table 6 [40,44].

The most critical step during the preparation of LLCs was the size reduction technique used. It majorly affects the size, size distribution, and entrapment efficiency. The smallest size was achieved with the probe sonication technique while screening different size reduction techniques. Techniques that provided the smallest to largest particle size were Probe sonication < High-speed mechanical stirring < Homogenization < Magnetic stirring < Low-speed mechanical stirring (Supplementary Table 2). No significant difference in the entrapment efficiency was observed in all these methods. However, probe sonication provided maximum entrapment value along with the smallest particle size. The critical process parameters are represented in Table 7.

4.1.4. Formulation of TMZ loaded LLCs

Formulating TMZ loaded LLCs by various methods revealed that the preparation method significantly affected the particle size and entrapment efficiency. When TMZ was added to the lipid phase, the solvent was required for solubilization of TMZ as it was not soluble in the lipid. The addition of acetone solubilized the drug but provided a lower entrapment value (up to 12%). In the next method, acetone was replaced with water as a solvent. TMZ was dissolved in a fixed quantity of water (about 20%) and added to the lipid phase. This also favored the self-assembly of the lipid molecules in presence of water. Allowing this phase to cool down to room temperature favored the formation of the lyotropic mesophase and also the entrapment of the TMZ molecules within. After cooling, this phase was subjected to size reduction. Immediate exposure to size reduction provided lower TMZ entrapment which may be attributed to the insufficient time provided for mesophase formation. This method significantly improved the entrapment efficiency of TMZ in LLCs (up to 30%). The concentration of water (Lipid to water ratio) plays an important role in forming the liquid crystal mesophase.

4.1.5. Experimental design for optimization and data analysis

Based on the preliminary trials, the variables selected were the amount of GMO (X1), amount of surfactant (X2), and amount of PEG 200 (X3) (Table 8). The dependent or response variables selected were mean particle size (Y1), PDI (Y2), zeta potential (Y3), % EE (Y4), and % DL (Y5). The variables were entered into the Box-Behnken design for the obtained 15 trials, including the

Table 1
Critical Quality Attributes of TMZ loaded LLCs.

Quality Target Product Profile (QTPP)	Impact analysis *	Severity analysis **	Is the quality attribute critical or not?	Justification
Dosage design	No	Yes (But is Already decided)	No	–
Dosage form	No	No (Is already decided)	No	–
Route of administration	No	Yes (But is Already decided)	No	–
Dosage strength	Yes	Yes	Yes	Affects the therapeutic effectiveness
Physical attributes	No	No	No	–
Assay	Yes	Yes	Yes	Affects the therapeutic effectiveness
pH of product	Yes	Yes	Yes	Affects the stability of drug and essential for parenteral administration
Particle size	Yes	Yes	Yes	Affects drug release rate, plasma circulation, and clearance rate
Zeta potential	Yes	Yes	Yes	Affects formulation stability, plasma circulation, protein binding, and uptake by organs
% Entrapment efficiency	Yes	Yes	Yes	Affects therapeutic effect
% Drug loading	Yes	Yes	Yes	Affects release rate and patient compliance
Drug release	Yes	Yes	Yes	Affects therapeutic effect and pharmacokinetic parameters
Pharmacokinetics	No	No	No	It is dependent on the other quality attributes
Stability	Yes	Yes	Yes	Affects therapeutic effect
Storage	No	Yes	No	–
Container closure system	No	Yes	No	–
Administration/ Labelling	No	Yes	No	–

*Does a change in formulation/process parameter affect the quality attribute of a product?
**Does failure to meet the quality attribute severely affect the efficacy and safety of the product in a patient?

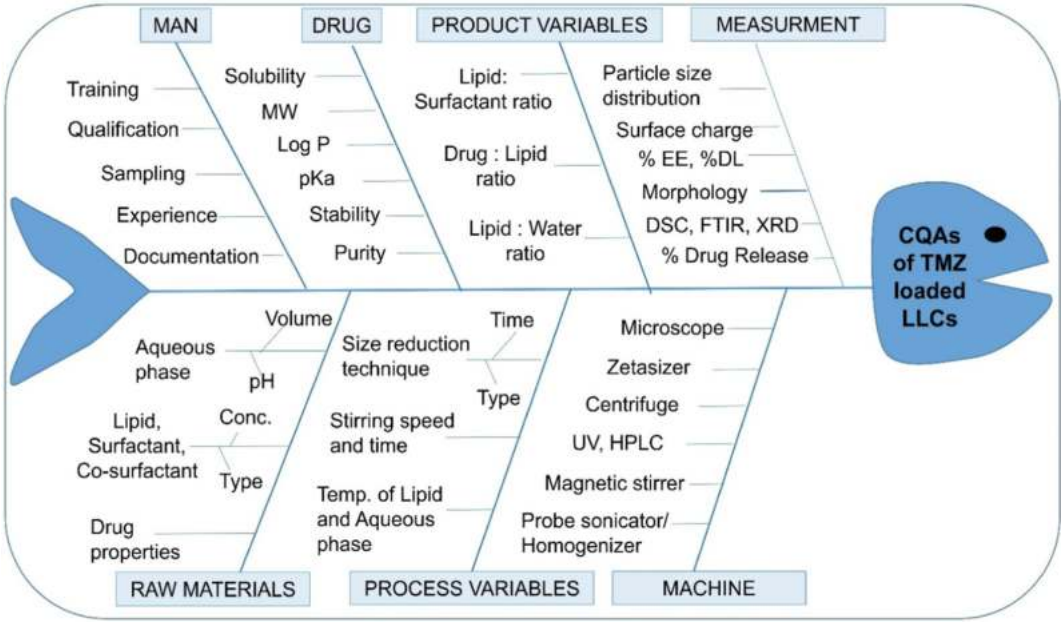

Fig. 1. Cause-effect analysis of TMZ loaded LLCs using the Fishbone diagram.

3 center points (CP) (Table 9). After statistical analysis, the obtained results were summarized in Table 10. The respective models for particle size, PDI, zeta potential, % EE, and % DL were found to be significant. The Lack of fit for the models was not significant [25,42].

4.1.6. Validation of the design and establishment of design space

The composition of the validation batches, predicted, and the observed values of the responses were represented in Table 11. The observed responses were found to be close to the predicted responses thus validating the model equations. The batch with GMO-300 mg, PF 127–150 mg, and PEG 200-1 mL was selected as the optimized batch for further studies as the highest entrapment and smallest particle size were achieved with the lowest lipid concentration. Design space was successfully established. The overlay plot is represented in Fig. 2 [45]

4.2. Characterization of TMZ loaded LLCs

4.2.1. Effect of formulation variables on particle size and PDI

The particle size of TMZ loaded LLCs was obtained between 53.157 and 186.500 nm. PDI was found to be 0.055–0.230. The polynomial equations obtained are represented as equations (6) and (7), respectively.

$$\text{Particle size}(Y1) = +156.04 + 45.02\ A - 25.06\ B - 22.69A^2 - 13.11\ B^2 \quad (6)$$

Table 2
Linking material attributes (MAs) of TMZ to Critical Quality Attributes (CQAs) of LLCs using relative risk-based matrix analysis.

MAs / CQAs	Solubility	Particle size	Moisture content	Chemical stability	Impurities
Assay					
pH of product					
Particle size distribution					
Zeta potential					
Entrapment and loading efficiency					
Drug release					
Stability					

Green: Low risk, Yellow: Medium risk, Red: High risk

Table 3
Linking material attributes (MAs) related to excipients to Critical Quality Attributes (CQAs) of LLCs using relative risk-based matrix analysis.

MAs / CQAs	Type of lipid	Hydro-phobicity of lipid	Melting point of lipid	Conc. of lipid	Conc. of surfactant/ stabilizer	pH of aqueous phase
Assay						
pH of product						
Particle size distribution						
Zeta potential						
Entrapment and loading efficiency						
Drug release						
Stability						

Green: Low risk, Yellow: Medium risk, Red: High risk

Table 4
Linking of process parameters (PPs) to Critical Quality Attributes (CQAs) of LLCs using relative risk-based matrix analysis.

PPs / CQAs	Temp. during stirring	Stirring Time	RPM of stirring	Size reduction technique	Parameters during size reduction (Temp., Time, Amplitude/Speed)
Assay					
pH of product					
Particle size distribution					
Zeta potential					
Entrapment and loading efficiency					
Drug release					
Stability					

Green: Low risk, Yellow: Medium risk, Red: High risk

Table 5
Failure mode effect analysis of material attributes of TMZ.

Material attribute	Failure mode	Effect on CQAs	P	S	D	RPN
Solubility	Low	Affect entrapment and loading efficiency-Drug release - Efficacy	3	5	2	**30**
Particle size	High	Affect content uniformity- Efficacy	2	2	1	4
Dose	High	Affect pharmacokinetic profile- Safety and Efficacy	3	4	1	12
Moisture content	High	Affect drug stability- Efficacy	2	3	2	12
Chemical Stability	Unstable	Affect assay and pharmacokinetic profile - Efficacy	4	5	2	**40**
Impurities	Present	Affect assay - safety and efficacy	2	4	2	16

Table 6
Failure mode effect analysis of the material attributes of the excipients used in the preparation of TMZ loaded LLCs.

Excipient	Material attribute	Failure mode	Effect on CQAs	P	S	D	RPN
Lipid	Type	Unsuitable for forming LLCs	Affect the formation of LLC- Surface charge-Safety and Efficacy	3	5	2	**30**
	Hydrophobicity	Low	Affect formation of LLC, and entrapment efficiency- Efficacy	2	4	2	16
	Melting point	Above 70 °C	Affect formation of LLC- Efficacy	2	3	1	6
	Concentration	High	Affect particle size, entrapment efficiency, drug release- Safety and Efficacy	3	5	2	**30**
Surfactant/Co-surfactant/ Stabilizer	Type	Unsuitable for forming LLCs	Affect formation of LLC- Surface charge-Safety and Efficacy	3	4	2	24
	Concentration	High	Affect particle size, entrapment efficiency, drug release, stability-Safety and Efficacy	4	4	2	**32**
Aqueous phase	pH	>5	Affect drug stability, and assay - Efficacy	3	5	2	**30**
	Volume	Low	Affect formation of LLC, entrapment efficiency, and drug release-Efficacy	3	4	1	12

Table 7
Failure mode effect analysis of process parameters involved in the preparation of TMZ loaded LLCs.

Process	Process parameters	Failure mode	Effect on CQAs	P	S	D	RPN
Magnetic stirring	Temperature	High	Affect phase formation-Drug degradation - Efficacy	2	4	2	16
	Time	High	Affect particle size distribution-Efficacy	3	2	1	6
	RPM	High	Affect particle size distribution-Efficacy	3	4	2	24
Size reduction technique	Type	Inadequate	Affect particle size distribution-Efficacy	4	4	1	16
	Temperature	High	Affect phase formation-Drug degradation - Efficacy	2	4	1	8
	Time	High	Affect particle size distribution-Efficacy	4	4	2	**32**
	Amplitude/ Pressure/ Speed	High	Affect particle size distribution-Efficacy	4	4	2	**32**

Table 8
Selected dependent variables and the response variables.

Factors	Units	Low (-1)	Medium (0)	High (+1)
GMO concentration (X1)	mg	200	500	800
PF 127 concentration (X2)	mg	50	100	150
PEG 200 concentration (X3)	mL	0.5	1.25	2
Responses and target goals				
Particle size (Y1)			Within range (80–120 nm)	
Polydispersity index (Y2)			Minimum	
Zeta potential (Y3)			Optimum	
% Entrapment efficiency (Y4)			Maximum	
% Drug loading (Y5)			Optimum	

$$PDI(Y2) = +0.16 - 0.024A + 0.043B + 0.00087C - 0.022B^2 + 0.033C^2 \quad (7)$$

In these equations, terms A, B, and C represent the factors X1, X2, and X3 respectively, '+' sign indicates a positive effect of the respective factor on the response variable while the '-' sign indicates the negative effect. The constant values before each term represent the quantitative effect on the response. Particle size was found to increase on increasing the lipid concentration, also denoted by the '+' sign of term A. Surfactant molecules occupy between the lipid molecules at the lipid water interface thus stabilizing the structure. When lipid concentration increases with a fixed amount of surfactant, fewer surfactant molecules are available per lipid molecule, increasing particle size. The surfactant molecules are not uniformly distributed among the lipid molecules, thus affecting the particle size and size distribution. The increasing number of surfactant molecules reduce the interfacial tension resulting in smaller sized particles as also indicated by the '-' sign of term B, and C. Particle size was found to be directly proportional to lipid concentration while inversely proportional to surfactant concentration as depicted by the perturbation plot and 3-D surface plot represented in Supplementary Fig. 1 (a) and Fig. 3 (a) respectively. The PEG 200 concentration was found to affect the PDI of the prepared formulations along with the PF127 concentration as represented in the perturbation (Supplementary Fig. 1 b) and 3-D surface plots (Fig. 3 b) [46,47].

4.2.2. Effect of formulation variables on zeta potential

The designed formulations expressed zeta potential in the range of −30.760 to −8.870 mV. The polynomial equation obtained for zeta potential is represented as equation (8).

$$\text{Zeta potential} = -17.95 - -6.72A \quad (8)$$

The results reflected that zeta potential was majorly dependent on the lipid concentration. GMO itself has a neutral surface charge. Commercial GMO contains free oleic acid that may contribute to the negative zeta potential. Also, the acidic pH of the medium may contribute to the zeta potential as the formulations were pre-

Table 9
Trials of Box-Behnken design along with the obtained responses.

Batch	X1 A:GMO(mg)	X2 B:PF 127(mg)	X3 C:PEG 200(mL)	Y1 Particle size(nm)	Y2 PDI	Y3 Zeta potential(mV)	Y4 % Entrapment efficency	Y5 % Drug loading
1	200	150	1.25	53.157 ± 1.08	0.218 ± 0.02	−14.867 ± 0.96	28.88 ± 0.38	0.753 ± 0.01
2	200	100	0.5	82.103 ± 1.12	0.196 ± 0.00	−13.034 ± 0.32	17.008 ± 0.36	0.594 ± 0.00
3	200	50	1.25	103.667 ± 1.19	0.127 ± 0.02	−9 ± 0.31	19.758 ± 0.63	0.77 ± 0.01
4	200	100	2	88.15 ± 1.72	0.23 ± 0.00	−8.87 ± 0.22	23.425 ± 0.48	0.79 ± 0.00
5 (CP)	500	100	1.25	162.134 ± 2.78	0.161 ± 0.01	−22 ± 0.10	26.87 ± 0.35	0.45 ± 0.00
6	500	150	2	116.67 ± 1.53	0.197 ± 0.00	−19.67 ± 0.28	33.67 ± 1.20	0.483 ± 0.00
7	500	150	0.5	117.8 ± 3.03	0.202 ± 0.00	−12.067 ± 0.15	34.21 ± 0.85	0.49 ± 0.03
8	500	50	0.5	171.467 ± 1.30	0.123 ± 0.02	−18.5 ± 1.13	33.45 ± 1.30	0.54 ± 0.05
9 (CP)	500	100	1.25	156.33 ± 1.76	0.14 ± 0.01	−19.9 ± 0.10	32.12 ± 2.01	0.5 ± 0.06
10 (CP)	500	100	1.25	150.466 ± 0.65	0.149 ± 0.00	−17.634 ± 0.41	28.23 ± 0.12	0.48 ± 0.08
11	500	50	2	164.934 ± 2.81	0.132 ± 0.02	−14.2 ± 1.05	31.673 ± 0.61	0.524 ± 0.01
12	800	100	0.5	182.267 ± 1.59	0.196 ± 0.00	−30.76 ± 0.77	32.19 ± 0.94	0.386 ± 0.02
13	800	100	2	180.033 ± 1.52	0.165 ± 0.01	−19.734 ± 0.32	25.72 ± 2.06	0.303 ± 0.02
14	800	150	1.25	138.434 ± 0.67	0.166 ± 0.02	−23.9 ± 0.88	29.56 ± 8.13	0.296 ± 0.02
15	800	50	1.25	186.5 ± 8.60	0.055 ± 0.05	−25.1 ± 1.12	32.53 ± 0.07	0.388 ± 0.00

Table 10
Summary of statistical parameters obtained for the responses.

Response	Significant model terms	F value	p-value Prob > F	
Y1 (Particle size)	Model	317.66	< 0.0001	Adj R-Squared: 0.9891
	A	871.31	< 0.0001	Pred R-Squared: 0.9828
	B	270.05	< 0.0001	Adeq Precision: 56.279
	A^2	102.77	< 0.0001	PRESS: 408.99
	B^2	34.31	0.0002	
Y2 (PDI)	Model	16.29	0.0003	Adj R-Squared: 0.8452
	A	14.11	0.0045	Pred R-Squared: 0.7011
	B	47.28	<0.0001	Adeq Precision: 13.032
	C	0.019	0.8924	PRESS: 8.554E-003
	B^2	5.59	0.0423	
	C^2	13.11	0.0056	
Y3 (Zeta potential)	Model	29.04	0.0001	Adj R-Squared: 0.6670
	A	29.04	0.0001	Pred R-Squared: 0.5797
				Adeq Precision: 10.436
				PRESS: 219.53
Y4 (% Entrapment efficiency)	Model	17.74	0.0006	Adj R-Squared: 0.8933
	A	41.00	0.0004	Pred R-Squared: 0.8205
	B	3.40	0.1077	Adeq Precision: 13.523
	C	0.24	0.6387	PRESS: 68.67
	AB	12.53	0.0095	
	AC	14.24	0.0070	
	A^2	32.73	0.0007	
	B^2	16.46	0.0048	
Y5 (% Drug loading)	Model	47.15	<0.0001	Adj R-Squared: 0.8683
	A	92.73	<0.0001	Pred R-Squared: 0.8201
	B	1.58	0.2332	Adeq Precision: 17.211
				PRESS: 0.061

Table 11
The composition of the validation batches, predicted, and the observed values.

GMO	270 mg		300 mg		320 mg	
PF 127	120 mg		150 mg		65 mg	
PEG 200	1.98 mL		1 mL		0.56 mL	
	Predicted	Observed	Predicted	Observed	Predicted	Observed
Size (nm)	96.52	119.20 ± 3.25	90	97.7 ± 0.481	132	149 ± 0.77
PDI	0.15	0.18 ± 0.00	0.19	0.18 ± 0.00	0.16	0.14 ± 0.02
% EE	27.46	21.78 ± 1.25	30.37	36.46 ± 1.48	23.47	22.41 ± 0.15

pared in acetate buffer (pH 4.5). The perturbation and 3-D surface plots obtained are represented in Supplementary Fig. 1 (c) and Fig. 3 (c), respectively [20,42].

4.2.3. Effect of formulation variables on entrapment efficiency and drug loading

The entrapment efficiency and drug loading of the prepared TMZ loaded LLCs were obtained between 17.008 and 34.210% and 0.296 and 0.790%, respectively. The polynomial equations obtained for the same are represented as equations (9) and (10), respectively.

$$\%\text{Entrapment efficiency} = +29.41 + 3.87A + 1.11B - 0.30C - 3.02AB - 3.22AC - 5.07A^2 + 3.60B^2 \quad (9)$$

$$\%\text{Drug Loading} = +0.52 - 0.19A - 0.025B \quad (10)$$

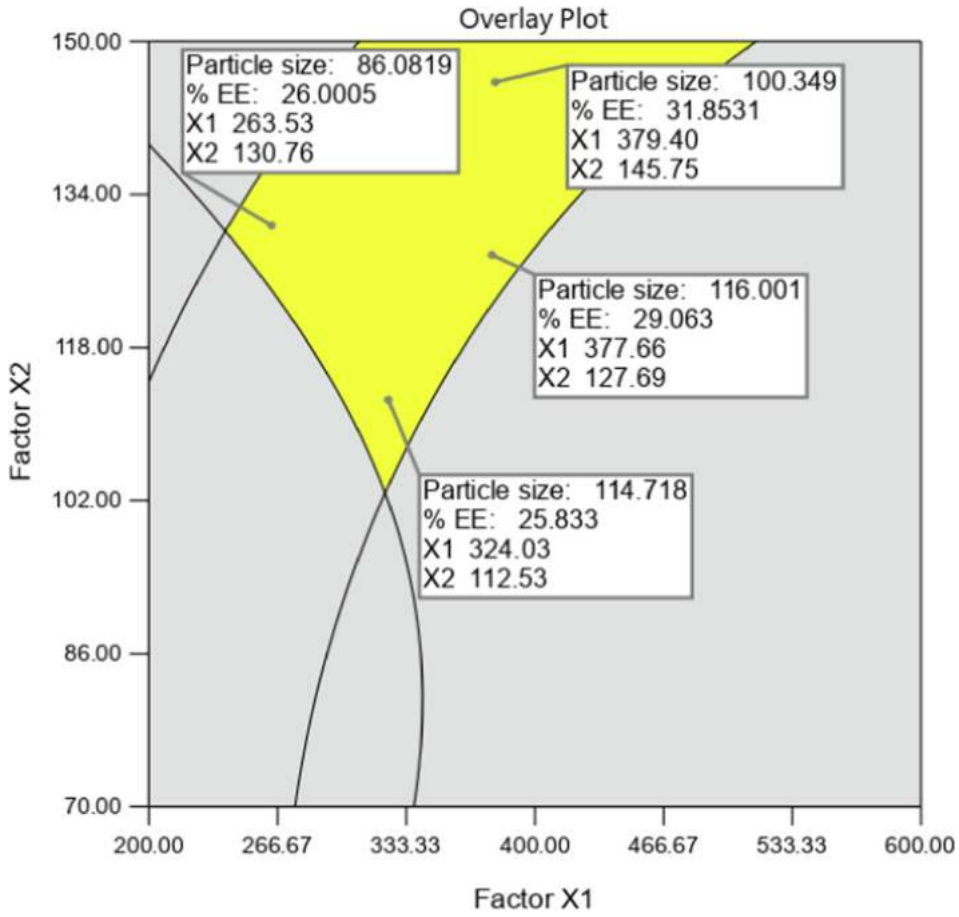

Fig. 2. Overlay plot representing design space to achieve target responses at medium level of X3 (PEG 200 concentration); Factor X1: GMO concentration; Factor X2: PF 127 concentration; % EE: % Entrapment efficiency.

In the above equations, the terms AB and AC represent the presence of the interaction effects between the respective factors. Entrapment efficiency was found to increase on increasing lipid concentration to a specific value, further increasing the lipid concentration demonstrated lower entrapment values (Supplementary Fig. 1 d and Fig. 3 d). Interaction between lipid and surfactant concentration was observed as the ratio of both has a significant effect on the particle size, ultimately affecting the entrapment efficiency. Drug loading was majorly dependent on the lipid concentration. As the lipid concentration increases for a fixed amount of drug concentration, more amount of lipid is present for a small amount of drug, thus reducing the % drug loading value (Supplementary Fig. 1e and Fig. 3e)[40,42].

4.2.4. Effect of PEG-200 and DSPE-PEG 2000 on the particle size distribution and zeta potential

The effect of PEG 200 and DSPE-PEG 2000 was studied by altering the concentration by keeping drug, lipid, and surfactant concentration constant. The results obtained are summarized in Table 12. It was found that PEG 200 concentration majorly affected the PDI. The PDI was found to increase in absence of PEG 200. DSPE-PEG 2000 is also reported to stabilize the LLC structure. PEG 200 was replaced with DSPE-PEG 2000 to overcome the hemolytic potential of GMO and also to improve the plasma circulation time. As the concentration of DSPE-PEG 2000 was increased from 0.05% to 1% of the total dispersion, particle size was found to reduce from 101.05 ± 1.202 nm to 85.27 ± 0.240 nm. DSPE-PEG 2000 may act as a surfactant and lower the particle size. PDI was found to increase on increasing concentrations of DSPE-PEG 2000. The particle size distribution graphs of the optimized formulations have been represented in Supplementary Fig. 2. The negatively charged functional groups in DSPE-PEG 2000 led to negative surface charge on LLCs [10,48].

4.2.5. Morphology

The lyotropic liquid crystal formation was confirmed by polarized light microscopy. Crystals have the property of birefringence and the ability to split the cross-polarized light. When we rotate the cross polarizer 90°, the appearance of bright crystals confirms the presence of lyotropic liquid crystals as represented in Fig. 4 a and b. The prepared formations had milk-like consistency and appearance depicting liquid nature. Thus the prepared LLCs had both crystalline and liquid-like properties. The SEM images confirmed the morphology of the formed LLCs. There was no change in morphology after PEGylation of the LLCs (Fig. 4 c and d) [42,49].

4.2.6. Atr-FTIR

The overlay of the FTIR spectrum is represented in Supplementary Fig. 3. For TMZ, characteristic peaks were observed at 3300 cm^{-1} (N-H band of secondary amide), 3350 and 3180 cm^{-1} (N-H stretch of primary amide observed as a doublet), 1680–1630 cm^{-1} (carbonyl amide), 1577 cm^{-1} (N = N stretching), and 1400 cm^{-1} (C-N stretching). In physical mixture and LLCs, prominent O-H stretch of alcohol between 3500 and 3200 cm^{-1}, =C-H bend of alkenes between 1000 and 650 cm^{-1} and C-H stretch of alkanes between 3000 and 2850 cm^{-1} was observed. In PEGylated LLCs, N-H bend of 1° amine between 1650 and 1580 cm^{-1} and prominent O-H stretch of alcohol between 3500 and 3200 cm^{-1}

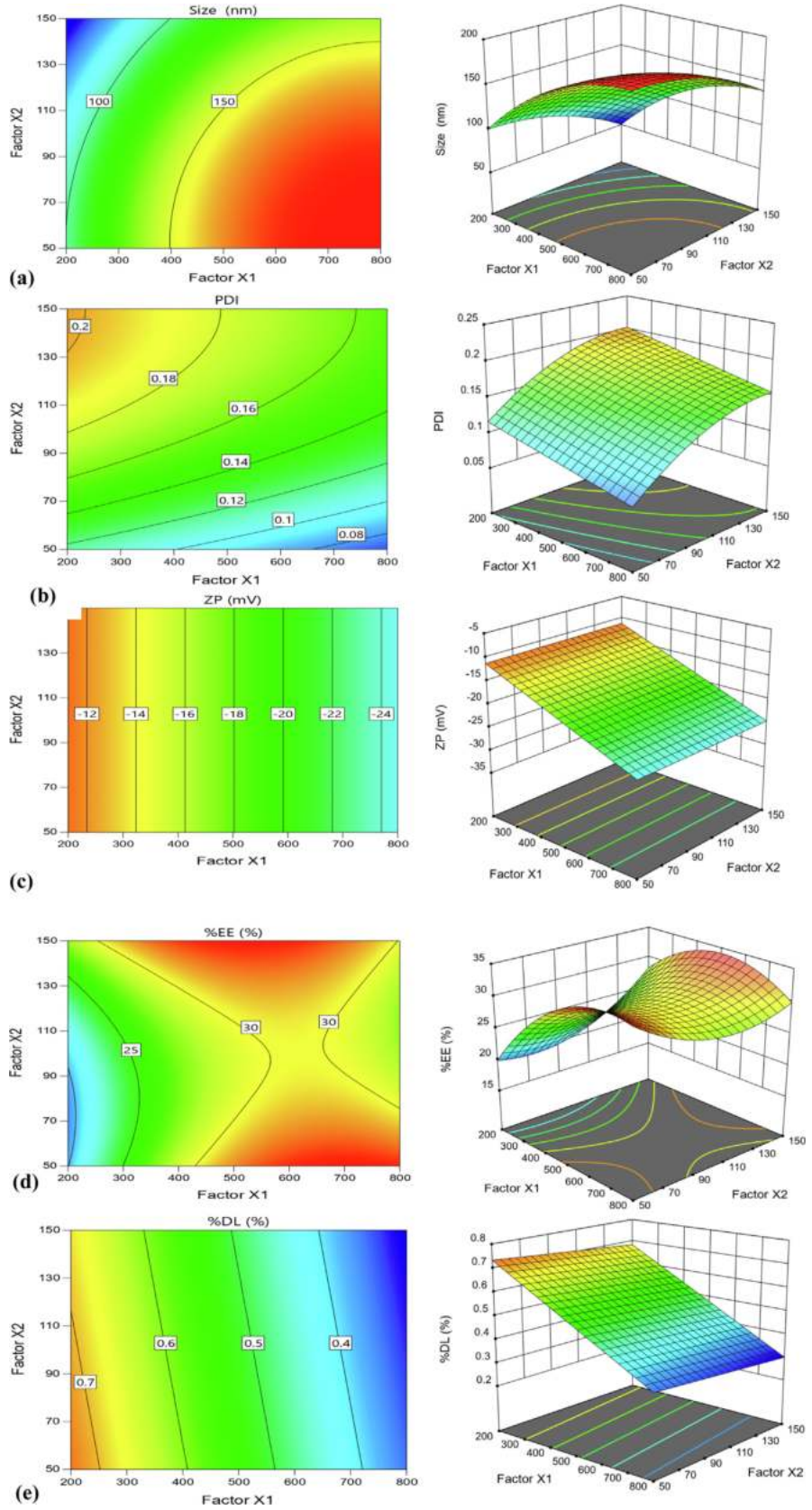

Fig. 3. Contour and 3D Surface plots (a) Particle size; (b) PDI; (c) Zeta potential; (d) % Entrapment efficiency; (e) % Drug Loading (Factor X1: GMO concentration; Factor X2: PF 127 concentration; All graphs represented at medium level of Factor X3: PEG 200 concentration).

Table 12
Effect of PEG 200 and DSPE-PEG 2000 on particle size, PDI, and zeta potential of LLCs (Measurements were done in triplicates for each formulation).

GMO (mg)	PF 127 (mg)	PEG 200 (mL)	DSPE-PEG 2000 (%)	Size (nm)	PDI	Zeta potential (mV)
300	150	0	0	110.15 ± 1.626	0.293 ± 0.013	−4.195 ± 0.134
300	150	1	0	111.05 ± 0.354	0.219 ± 0.013	−1.48 ± 0.474
300	150	0	0.05	101.05 ± 1.202	0.241 ± 0.003	−6.29 ± 0.226
300	150	0	0.1	94.475 ± 1.817	0.259 ± 0.014	−9.48 ± 0.106
300	150	0	0.25	94.785 ± 6.286	0.282 ± 0.003	−11.7 ± 1.768
300	150	0	0.5	90.29 ± 1.117	0.359 ± 0.001	−16.7 ± 0.283
300	150	0	1	85.27 ± 0.240	0.297 ± 0.004	−25.05 ± 1.768

*DSPE-PEG 2000 represented as % (w/v) of the total dispersion (10 mL)

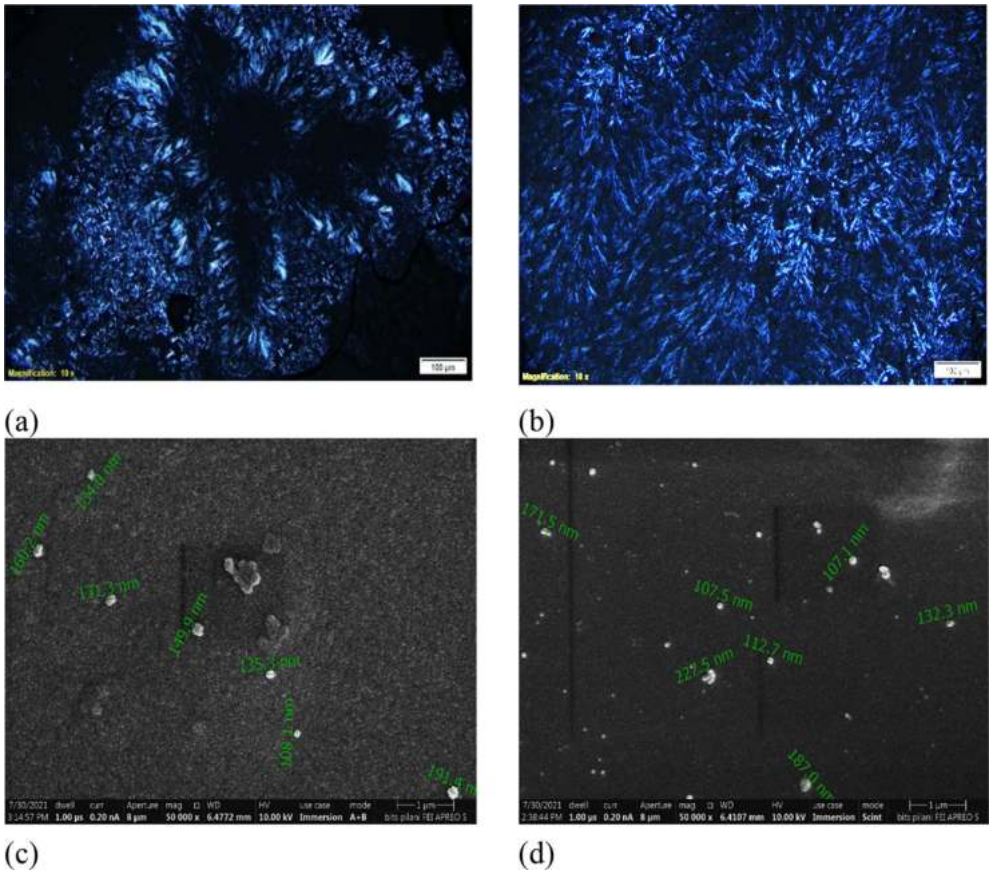

Fig. 4. Morphology of LLCs. (a) Polarized light microscopy image of TMZ loaded LLCs with the cross polarizer; (b) PEGylated TMZ loaded LLCs with the cross polarizer; (c) SEM image of TMZ loaded LLCs; (d) SEM image of PEGylated TMZ loaded LLCs.

was observed. No major interaction between TMZ and the excipients was detected.

4.2.7. XRD

The XRD diffractogram of TMZ, Physical mixture, and TMZ loaded PEGylated LLCs is represented in Fig. 5. Sharp narrow peaks indicate that the substance is crystalline, while broad peaks represent amorphous nature. Sharp peaks were observed at 10.83, 14.63, 17.98, 19.05, 26.49, and 29.80°in the TMZ diffractogram, revealing the crystalline nature of the drug. The intense sharp peaks of TMZ disappeared in the diffractogram of LLCs, indicating drug entrapment inside the LLCs. New sharp peaks at 20.65, 25.46, and 36.39°appeared in diffractogram of LLCs, revealing the crystalline nature of the LLCs, which confirmed the formation of a liquid crystal structure.

4.2.8. Drug release and release kinetics

In-vitro drug release showed that the free drug was found to show 100% diffusion within 2 h and followed first-order release kinetics, where as TMZ loaded LLCs exhibited sustained release up to more than 72 h. The drug release profile obtained is represented in Fig. 6. The drug crosses multiple layers before reaching the outside media, thus leading to the slow release of the drug. The release of TMZ from LLCs could be explained by Korsmeyer's Peppas model. The release exponent 'n' value<0.45 demonstrated diffusion-controlled drug release. The release kinetics parameters of the best fit model for TMZ and TMZ loaded LLCs are summarized in Table 13. The drug release rate was found to be proportional to the drug loading and followed the same model. The higher the lipid concentration, the slower the drug release rate as the entrapped drug has to diffuse through the channels of the lipid matrix [8,42].

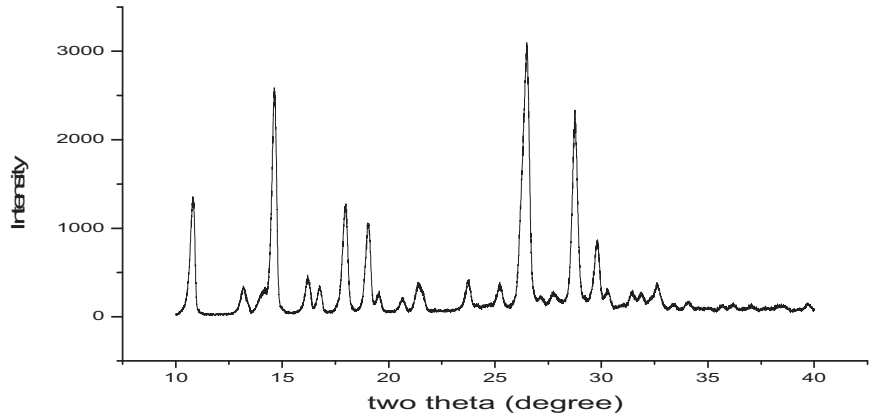

(a) TMZ

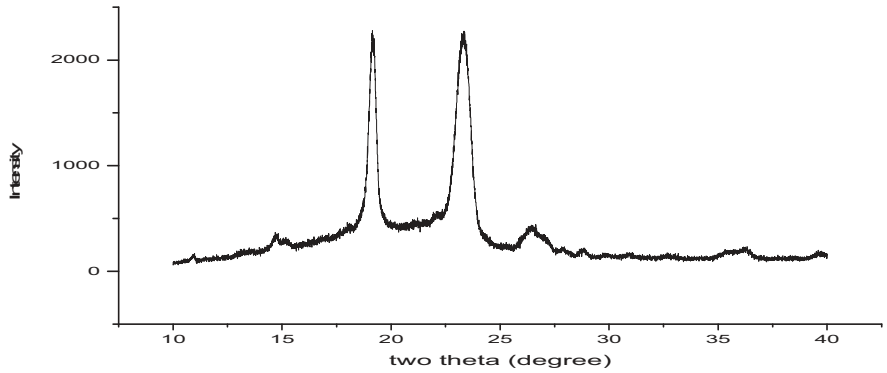

(b) Physical mixture

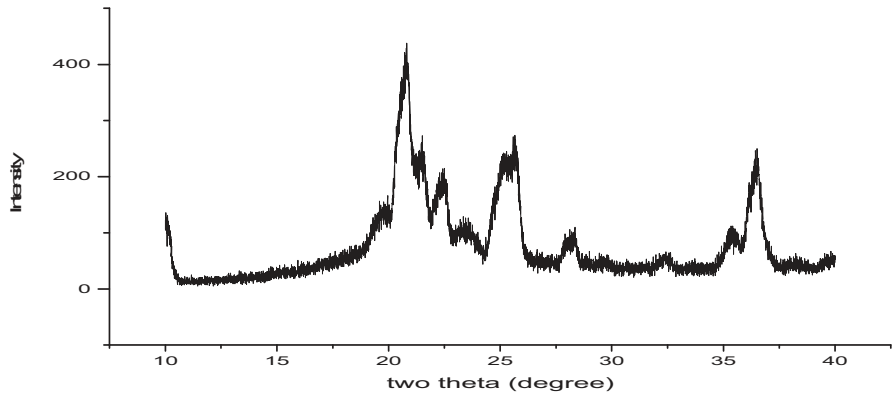

(c) TMZ loaded PEGylated LLCs

Fig. 5. XRD diffractogram of (a) TMZ, (b) Physical mixture, and (c) TMZ loaded PEGylated LLCs.

4.2.9. Hemolysis study

GMO-based formulations are reported to cause hemolysis. GMO-containing LLCs were found to show about 47.42 ± 2.26% hemolysis (Fig. 7). They were found to show 6.66 ± 1.90% hemolysis even after 10 times dilution. In addition to GMO, DSPE-PEG 2000 was added to the formulation to overcome the hemolysis. It was observed that increasing the concentration of DSPE-PEG 2000 from 0.05% to 1% significantly reduced the hemolysis of RBCs. LLCs containing 1% DSPE-PEG 2000 with and without dilution were found to show less than 5% hemolysis. This study proved the potential of PEGylated LLCs containing 1% DSPE-PEG 2000 for administration into the systemic circulation. PEG 2000 molecules adsorbed on the surface prevent the interaction with the RBCs, thus the subsequent hemolysis [10,20].

4.2.10. In-vitro cytotoxicity study

MTT assay is one of the colorimetric tests used to assess cell viability. The cellular enzymes metabolize the MTT dye to formazan

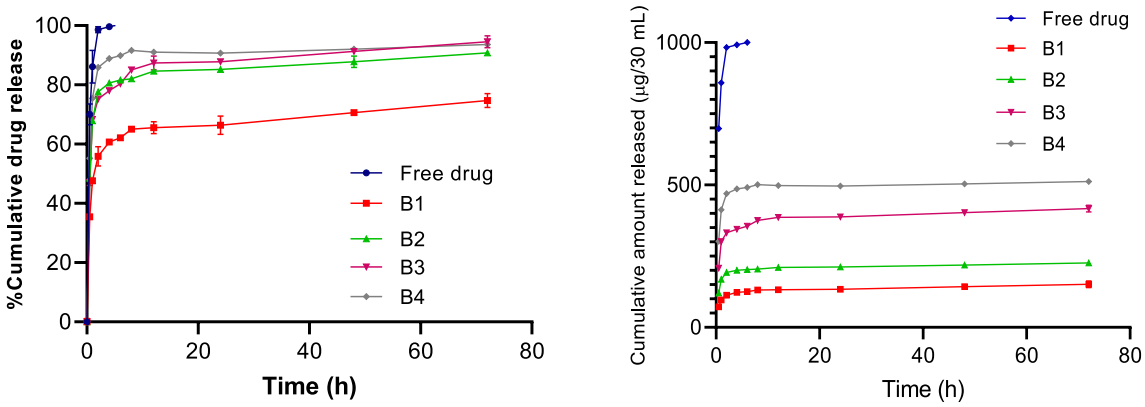

Fig. 6. Drug release profile of TMZ and TMZ loaded LLCs with different drug loading (B1- 0.45 %, B2- 0.72 %, B3- 1.00 %, B4- 1.52%) (n = 3 represented as Mean ± SD).

Table 13
Various release kinetics parameters of the best fit model for TMZ and TMZ loaded LLCs.

Free drug	**B1**	**B2**	**B3**	**B4**
Model	**First order**	**Korsmeyer-Peppas**		
K	2.266	47.562	67.042	66.501	75.964
n					
n	-	0.121	0.080	0.086	0.057
R2	0.9989	0.9824	0.9777	0.9795	0.9694
AIC	19.187	74.581	80.798	80.348	85.297
MSC	4.314	2.245	1.637	1.792	1.077
t_{25}	0.127	0.005	0.000	0.000	0.000
t_{50}	0.306	1.511	0.026	0.037	0.001
t_{75}	0.612	43.083	4.060	4.026	0.799

crystals. Dead cells are not able to metabolize due to the absence of enzymes. When solubilized in DMSO, the formazan crystals produce purple color that has characteristic absorption at 570 nm. The results obtained for cell viability are summarized in Fig. 8. TMZ was found to show dose-dependent cytotoxicity on glioma cells. The IC50 value for TMZ was found to be 0.74 mM. TMZ loaded LLCs were found to show significantly increased cell cytotoxicity. The TMZ loaded LLCs and TMZ loaded PEGylated LLCs showed IC50 values of 0.06 mM and 0.48 mM, respectively. TMZ loaded LLCs and TMZ loaded PEGylated LLCs were found to show 12.33 and 1.54 fold more cytotoxicity as compared to TMZ alone. The lipidic, bioadhesive and membrane fusing nature of GMO helps improve cell internationalization. As the drug concentration increases, the number of LLCs also increases, ultimately resulting in higher cytotoxicity. PEGylated LLCs showed less cytotoxicity as compared to LLCs. This may be attributed to the negative surface charge of PEGylated LLCs, leading to less affinity towards negative cell surface, thus less cell uptake. The study revealed that incorporating TMZ into the LLCs potentiates the cytotoxicity of TMZ [10].

4.3. Reproducibility and scale-up studies

The average particle size and PDI of the 6 repeated batches were found to be 98.98 ± 7.14 nm and 0.195 ± 0.01, respectively, which confirmed that the process was highly reproducible. To prepare the 50 mL batch, the beaker size and the probe size were increased proportionally, and the sonication time was optimized. The particle size and PDI obtained for the scale-up batch were 120.8 ± 0.70 and 0.219 ± 0.003, respectively. As the process involved a minimum number of steps, it was feasible for scale-up. The particle size and PDI of both LLCs and PEGylated LLCs were found to be stable even after 1000 times dilution, which revealed that the structure was maintained even after dilution (Fig. 9). The particle size data quality report has been represented in the Supplementary Table 3 [24].

5. Conclusion

TMZ loaded LLCs were successfully optimized using the principles of Quality by Design. Understanding the effect of various material attributes and the process parameters on the critical quality attributes is essential and lowers the risk of product failure. The unique structure of LLCs allows entrapment of amphiphilic drug-like TMZ and provides controlled release. PEGylation of LLCs significantly overcomes the hemolytic potential of GMO. The system has the potential to enhance the plasma circulation time of TMZ and thus improve brain bioavailability. The preparation method involved the minimum number of steps, was highly reproducible and industrially feasible.

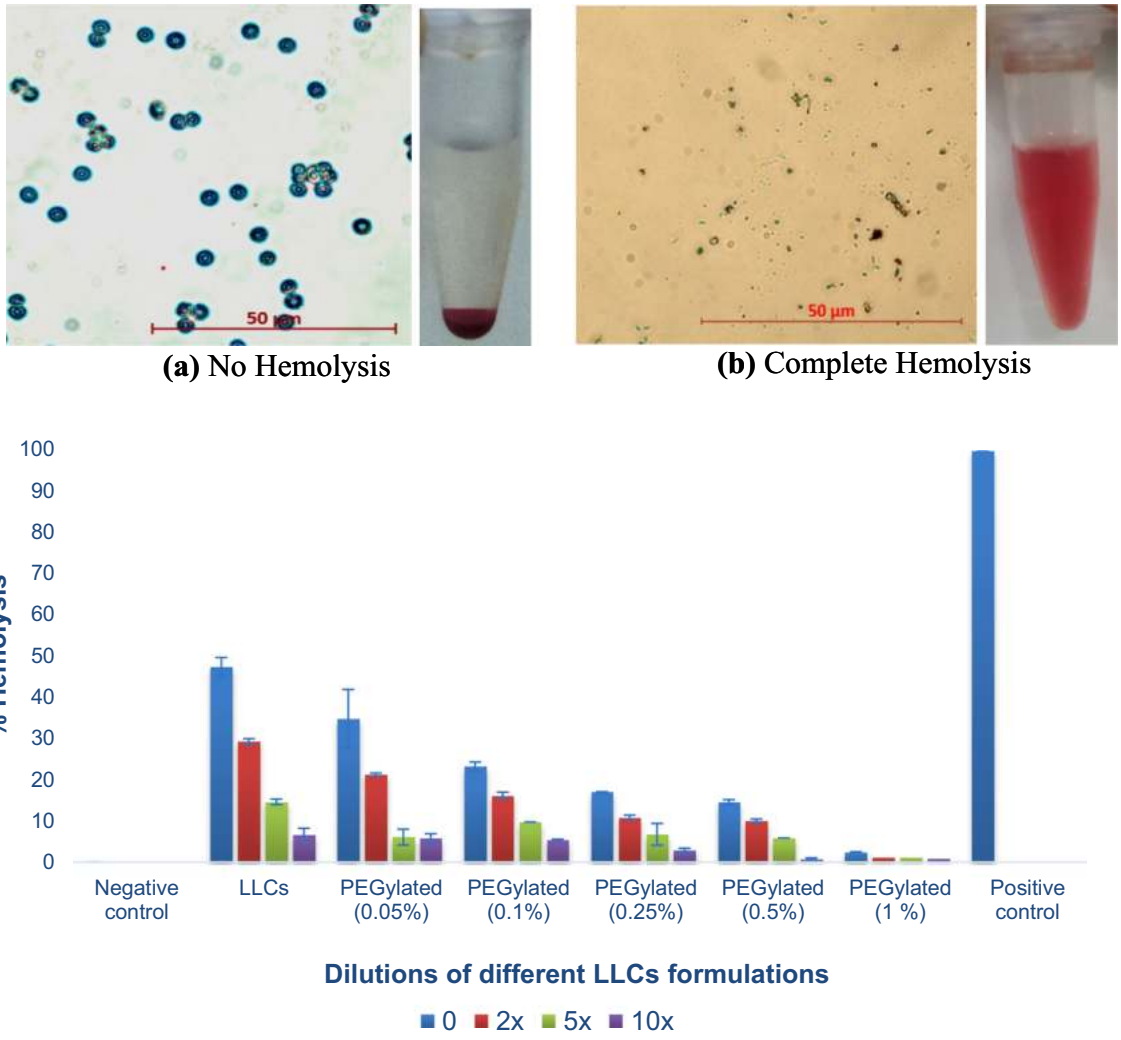

Fig. 7. Fluorescence microscopic image of (a) intact RBCs indicating no hemolysis; (b) RBCs after hemolysis;and (c) % Hemolysis of different LLCs formulations. The % values in brackets represent the DSPE-PEG 2000% w/v in the PEGylated LLCs. The dilution medium used was normal saline (n = 3 represented as Mean ± SD).

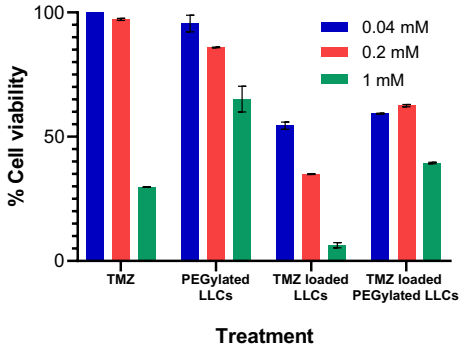

Fig. 8. In-vitro cytotoxicity assessment of TMZ and TMZ loaded LLCs on U-373 MG cells exposed for 48 h. Data represented as Mean ± SD (n = 4, where n represents number of wells in an experiment).

Funding

This research did not receive any specific grant from funding agencies in the public, commercial, or not-for-profit sectors

CRediT authorship contribution statement

Tejashree Waghule: Methodology, Investigation, Writing – original draft. **K. Laxmi Swetha:** Methodology. **Aniruddha Roy:** Data curation, Validation. **Ranendra Narayan Saha:** Project administration, Supervision. **Gautam Singhvi:** Conceptualization, Investigation, Project administration, Writing – review & editing.

Declaration of Competing Interest

The authors declare that they have no known competing financial interests or personal relationships that could have appeared to influence the work reported in this paper.

Acknowledgement

Authors are very thankful to Biophore India Pharmaceuticals Pvt Ltd (Hyderabad) for providing a generous gift sample of temozolomide. We are thankful to Mohini Organics Pvt. Ltd. for providing us Glyceryl monooleate (Monegyl-O100) as a gift sample for this research study. We acknowledge the research support of BASF (India) for providing a gift sample of Pluronic 127. We highly

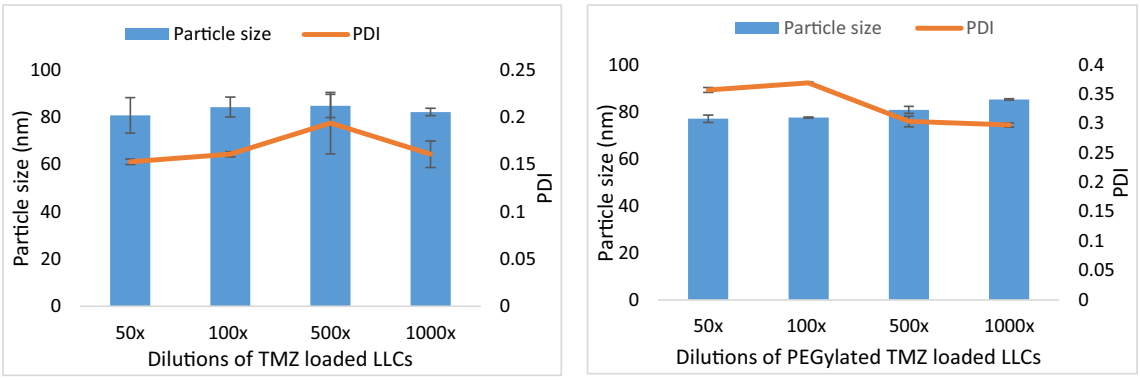

Fig. 9. Particle size (nm) and PDI of TMZ loaded LLCs and PEGylated LLCs on different dilutions with Milli Q water. The zeta potential of TMZ loaded LLCs and PEGylated LLCs was found to be −6.49 ± 2.19 mV and 18.24 ± 6.42 mV respectively (n = 3 shown as Mean ± SD).

appreciate the kind support of Lipoid for providing DSPE-PEG 2000 as a gift sample. We acknowledge the support of DST, Prof. Anshuman Dalvi, and group, Department of Physics, BITS PILANI, Pilani campus for supporting XRD analysis.

Appendix A. Supplementary data

Supplementary data to this article can be found online at https://doi.org/10.1016/j.molliq.2022.118724.

References

[1] I.C. Lopes, S.C.B. de Oliveira, A.M. Oliveira-Brett, Temozolomide chemical degradation to 5-aminoimidazole-4-carboxamide – Electrochemical study, J. Electroanal. Chem. 704 (2013) 183–189.
[2] S.J. Danson, M.R. Middleton, Temozolomide: a novel oral alkylating agent, Exp. Rev. Anticancer Therapy (2001) 13–19.
[3] E.S. Newlands, G.R.P. Blackledge, J.A. Slack, G.J.S. Rustin, D.B. Smith, N.S.A. Stuart, et al., Phase I trial of temozolomide (CCRG 81045: M & B 39831: NSC 362856), Br. J. Cancer. (1992) 287–291.
[4] J. Qu, L. Zhang, Z. Chen, G. Mao, Z. Gao, J. Qu, et al., Nanostructured lipid carriers, solid lipid nanoparticles, and polymeric nanoparticles : which kind of drug delivery system is better for glioblastoma chemotherapy ? Nanostructured lipid carriers, solid lipid nanoparticles, and polymeric nanoparticles, Drug Deliv. 23 (9) (2016) 3408–3416.
[5] J. Gao, Z. Wang, H. Liu, L. Wang, G. Huang, Liposome encapsulated of temozolomide for the treatment of glioma tumor: preparation, characterization and evaluation, Drug Discov. Ther. 9 (3) (2015) 205–212.
[6] C. Kalyani Ashok, M. Ola, D.R. Ramesh, V.A. Chaudhari, Liquid crystals: A review, Int. J. Creat Innov. Res. All. Stud. 1 (12) (2019) 119–129.
[7] S. Gaballa, O. El Garhy, H. Abdelkader, Cubosomes: composition, preparation, and drug delivery applications, J. Adv. Biomed. Pharm. Sci. 3 (2020) 1–9.
[8] T. Waghule, V.K. Rapalli, G. Singhvi, S. Gorantla, A. Khosa, S.K. Dubey, et al., Design of temozolomide-loaded proliposomes and lipid crystal nanoparticles with industrial feasible approaches: comparative assessment of drug loading, entrapment efficiency, and stability at plasma pH, J. Liposome Res. (2020) 1–11.
[9] G. Singhvi, S. Banerjee, A. Khosa, Lyotropic liquid crystal nanoparticles: A novel improved lipidic drug delivery system, in: A.M. Grumezescu (Ed.), Organic Materials as Smart Nanocarriers for Drug Delivery, William Andrew Publishing, UK, 2018, pp. 471–517.
[10] F. May, Y.S.R. Elnaggar, A.A. Doaa, A.Y.O. Stealth, biocompatible monoolein-based lyotropic liquid crystalline nanoparticles for enhanced aloe-emodin delivery to breast cancer cells : in vitro and in vivo studies, Int. J. Nanomed. 11 (2016) 4799–4818.
[11] Z. Niu, I. Conejos-Sánchez, B.T. Griffin, C.M. O'Driscoll, M.J. Alonso, Lipid-based nanocarriers for oral peptide delivery, Adv. Drug Deliv. Rev. 106 (2016) 337–354.
[12] V.K. Rapalli, T. Waghule, N. Hans, A. Mahmood, S. Gorantla, S.K. Dubey, G. Singhvi, Insights of lyotropic liquid crystals in topical drug delivery for targeting various skin disorders, J. Mol. Liq. 315 (2020) 113771, https://doi.org/10.1016/j.molliq.2020.113771.
[13] V.K. Rapalli, A. Khosa, G. Singhvi, V. Girdhar, R. Jain, S.K. Dubey, Application of QbD Principles in Nanocarrier-Based Drug Delivery Systems, in: M.S.H. Sarwar Beg (Ed.), Pharmaceutical Quality by Design, Academic Press, 2019, pp. 255–296.
[14] D. Soans, R. Chandramouli, A.N. Kavitha, S.K.S.S. Roopesh, Application of design of experiments for optimizing critical quality attributes (CQA) in routine, J. Pharm. Res. 15 (3) (2016) 96–100.
[15] M.N. Javed, M.S. Alam, A. Waziri, F.H. Pottoo, A.K. Yadav, M.S. Hasnain, et al., QbD Applications for the Development of Nanopharmaceutical Products, Pharm Qual by Des. (March) (2019) 229–253.
[16] N.S.K. Srinivas, R. Verma, G.P. Kulyadi, L. Kumar, A quality by design approach on polymeric nanocarrier delivery of gefitinib: Formulation, in vitro, and in vivo characterization, Int. J. Nanomed. 12 (2017) 15–28.
[17] N.K. Garg, G. Sharma, B. Singh, P. Nirbhavane, R.K. Tyagi, R. Shukla, O.P. Katare, Quality by Design (QbD)-enabled development of aceclofenac loaded-nano structured lipid carriers (NLCs): An improved dermatokinetic profile for inflammatory disorder(s), Int. J. Pharm. 517 (1-2) (2017) 413–431.
[18] L. Zhang, S. Mao, Application of quality by design in the current drug development, Asian J. Pharm. Sci. 12 (1) (2017) 1–8.
[19] M. Nasr, M.K. Ghorab, A. Abdelazem, In vitro and in vivo evaluation of cubosomes containing 5-fluorouracil for liver targeting, Acta Pharm. Sin. B. 5 (1) (2015) 79–88.
[20] V. Jain, N.K. Swarnakar, P.R. Mishra, A. Verma, A. Kaul, A.K. Mishra, N.K. Jain, Paclitaxel loaded PEGylated gleceryl monooleate based nanoparticulate carriers in chemotherapy, Biomaterials 33 (29) (2012) 7206–7220.
[21] S. Ranga, M. Jaimini, S.K. Sharma, B.S. Chauhan, A. Kumar, A Review on Design OF Experiments (DOE), Int. J. Pharm. Chem. Sci. 3 (1) (2014) 216–224.
[22] T. Waghule, V.K. Rapalli, G. Singhvi, P. Manchanda, N. Hans, S.K. Dubey, M.S. Hasnain, A.K. Nayak, Voriconazole loaded nanostructured lipid carriers based topical delivery system: QbD based designing, characterization, in-vitro and ex-vivo evaluation, J. Drug Deliv. Sci. Technol. 52 (2019) 303–315.
[23] S. Chaudhary, A DoE / QbD Optimization Model of "DRY MIXING-DIRECT COMPRESSION" Process using 3^2 Full factorial Design for Solid Oral Dosage Forms, Int. J. Pharm. (July) (2018).
[24] V.K. Rapalli, S. Sharma, A. Roy, G. Singhvi, Design and dermatokinetic evaluation of Apremilast loaded nanostructured lipid carriers embedded gel for topical delivery: A potential approach for improved permeation and prolong skin deposition, Colloids Surfaces B Biointerfaces. 206 (2021) 111945, https://doi.org/10.1016/j.colsurfb.2021.111945.
[25] D. Bei, J. Marszalek, B.C. Youan, Formulation of Dacarbazine-loaded Cubosomes — Part II : In fl uence of Process Parameters, AAPS PharmSciTech. 10 (3) (2009) 1040–1047.
[26] J. Merlo-Mas, J. Tomsen-Melero, J.-L. Corchero, E. González-Mira, A. Font, J.N. Pedersen, N. García-Aranda, E. Cristóbal-Lecina, M. Alcaina-Hernando, R. Mendoza, E. Garcia-Fruitós, T. Lizarraga, S. Resch, C. Schimpel, A. Falk, D. Pulido, M. Royo, S. Schwartz, I. Abasolo, J.S. Pedersen, D. Danino, A. Soldevila, J. Veciana, S. Sala, N. Ventosa, A. Córdoba, Application of Quality by Design to the robust preparation of a liposomal GLA formulation by DELOS-susp method, J. Supercrit. Fluids 173 (2021) 105204, https://doi.org/10.1016/j.supflu.2021.105204.
[27] S. Bhattacharjee, DLS and zeta potential - What they are and what they are not?, J Control. Release 235 (2016) 337–351.
[28] P. Zhang, T. Jing, J. Zhang, Preparation, characterization, and evaluation of amphotericin B-loaded MPEG-PCL-g-PEI micelles for local treatment of oral Candida albicans, Int. J. Nanomed. 12 (2017) 4269–4283.
[29] M. Pradhan, D. Singh, S.N. Murthy, M.R. Singh, Design, characterization and skin permeating potential of Fluocinolone acetonide loaded nanostructured lipid carriers for topical treatment of psoriasis, Steroids 101 (2015) 56–63.
[30] S. Omar, A. Ismail, K. Hassanin, S. Hamdy, Formulation and Evaluation of Cubosomes as Skin Retentive System for Topical Delivery of Clotrimazole, J. Adv. Pharm. Res. 3 (2) (2019) 68–82.
[31] M. Płaczek, M. Kosela, Microscopic methods in analysis of submicron phospholipid dispersions, Acta Pharm. 66 (1) (2016) 1–22.
[32] A. Sharma, A. Sood, V. Mehta, U. Malairaman, Formulation and Physicochemical Evaluation of Nanostructured Lipid Carrier for Codelivery of Clotrimazole and Ciprofloxacin, Asian J. Pharm. Clin. Res. 9 (3) (2016) 356–360.
[33] E. Esposito, P. Mariani, M. Drechsler, R. Cortesi, Structural Studies of Lipid-Based Nanosystems for Drug Delivery: X-ray Diffraction (XRD) and Cryogenic Transmission Electron Microscopy (Cryo-TEM), in: M. Aliofkhazraei (Ed.),

Handbook of Nanoparticles, Springer International Publishing, Cham, pp. 1–23, https://doi.org/10.1007/978-3-319-13188-7_39-1.
[34] L. Zhao, H. Xiong, H. Peng, PEG-coated lyophilized proliposomes : preparation, characterizations and in vitro release evaluation of vitamin E, Eur. Food Res. Technol. 232 (2011) 647–654.
[35] A. Mahmood, V. Krishna, T. Waghule, S. Gorantla, S. Kumar, R. Narayan, et al., Spectrochimica Acta Part A : Molecular and Biomolecular Spectroscopy UV spectrophotometric method for simultaneous estimation of betamethasone valerate and tazarotene with absorption factor method : Application for in-vitro and ex-vivo characterization of, Spectrochim. Acta Part A Mol. Biomol. Spectrosc. 235 (2020) 118310.
[36] J. Zuo, Y. Gao, N. Bou-Chacra, R. Löbenberg, Evaluation of the DDSolver software applications, Biomed Res. Int. 2014 (2014).
[37] Y. Zhang, M. Huo, J. Zhou, A. Zou, W. Li, C. Yao, et al., DDSolver: An add-in program for modeling and comparison of drug dissolution profiles, AAPS J. 12 (3) (2010) 263–271.
[38] D.H. Surve, Y.B. Jirwankar, V.D. Dighe, A.B. Jindal, Long-Acting Efavirenz and HIV - 1 Fusion Inhibitor Peptide Co-loaded Polymer – Lipid Hybrid Nanoparticles: Statistical Optimization, Cellular Uptake, and In Vivo Biodistribution, Mol. Pharm. 17 (2020) 3990–4003.
[39] B.K. Patel, R.H. Parikh, Formulation development and evaluation of temozolomide loaded hydrogenated soya phosphatidylcholine liposomes for the treatment of brain cancer, Asian J. Pharm. Clin. Res. 9 (3) (2016), 340–340.
[40] S. Gorantla, R.N. Saha, G. Singhvi, Exploring the affluent potential of glyceryl mono oleate – myristol liquid crystal nanoparticles mediated localized topical delivery of Tofacitinib: Study of systematic QbD, skin deposition and dermal pharmacokinetics assessment, J. Mol. Liq. 346 (2022) 117053.
[41] J. Lu, S.C. Owen, M.S. Shoichet, Stability of self-assembled polymeric micelles in serum, Macromolecules 44 (15) (2011) 6002–6008.
[42] T. Waghule, S. Patil, V.K. Rapalli, V. Girdhar, S. Gorantla, S. Kumar Dubey, et al., Improved skin-permeated diclofenac-loaded lyotropic liquid crystal nanoparticles: QbD-driven industrial feasible process and assessment of skin deposition, Liq. Cryst. 47 (2020) 1–19.
[43] A. Mahmood, V.K. Rapalli, T. Waghule, S. Gorantla, G. Singhvi, Luliconazole loaded lyotropic liquid crystalline nanoparticles for topical delivery: QbD driven optimization, in-vitro characterization and dermatokinetic assessment, Chem. Phys. Lipids 234 (2021) e105028.
[44] T. Waghule, N. Dabholkar, S. Gorantla, V.K. Rapalli, R.N. Saha, G. Singhvi, Quality by design (QbD) in the formulation and optimization of liquid crystalline nanoparticles (LCNPs): A risk based industrial approach, Biomed. Pharmacother. 141 (2021).
[45] M. Patel, K. Sawant, A Quality by Design Concept on Lipid Based Nanoformulation Containing Antipsychotic Drug: Screening Design and Optimization using Response Surface Methodology, J Text Sci Eng. 08 (03) (2017) 1000442.
[46] D. Bei, J. Marszalek, B.C. Youan, Formulation of Dacarbazine-Loaded Cubosomes — Part I : In fl uence of Formulation Variables, AAPS PharmSciTech. 10 (3) (2009) 1032–1039.
[47] H.M. Abdelaziz, O. Elzoghby, W. Maged, M.W. Samaha, J. Fang, S. May, Liquid crystalline assembly for potential combinatorial chemo – herbal drug delivery to lung cancer cells, Int. J. Nanomed. 14 (2019) 499–517.
[48] J. Zhai, T.M. Hinton, L.J. Waddington, C. Fong, N. Tran, X. Mulet, et al., Lipid – PEG Conjugates Sterically Stabilize and Reduce the Toxicity of Phytantriol-Based Lyotropic Liquid Crystalline Nanoparticles, Langmuir 31 (2015) 10871–10880.
[49] X. Wang, Y. Zhang, S. Gui, J. Huang, J. Cao, Z. Li, et al., Characterization of Lipid-Based Lyotropic Liquid Crystal and Effects of Guest Molecules on Its Microstructure: a Systematic Review, AAPS PharmSciTech. 19 (5) (2018) 2023–2040.